Energy-Efficient Symbol-Level Precoding in Multiuser MISO Based on Relaxed Detection Region

Maha Alodeh, *Member, IEEE*, Symeon Chatzinotas, *Senior Member, IEEE,* Björn Ottersten, *Fellow Member, IEEE*

***Abstract*—This paper addresses the problem of exploiting interference among simultaneous multiuser transmissions in the downlink of multiple-antenna systems. Using symbol-level precoding, a new approach towards addressing the multiuser interference is discussed through jointly utilizing the channel state information (CSI) and data information (DI). The interference among the data streams is transformed under certain conditions to a useful signal that can improve the signal-to-interference noise ratio (SINR) of the downlink transmissions and as a result the system's energy efficiency. In this context, new constructive interference precoding techniques that tackle the transmit power minimization (min power) with individual SINR constraints at each user's receiver have been proposed. In this paper, we generalize the constructive interference (CI) precoding design under the assumption that the received MPSK symbol can reside in a relaxed region in order to be correctly detected. Moreover, a weighted maximization of the minimum SNR among all users is studied taking into account the relaxed detection region. Symbol error rate analysis (SER) for the proposed precoding is discussed to characterize the trade-off between transmit power reduction and SER increase due to the relaxation. Based on this trade-off, the energy efficiency performance of the proposed technique is analyzed. Finally, extensive numerical results show that the proposed schemes outperform other state-of-the-art techniques.**

***Index Terms*—Constructive interference, multiuser MISO, relaxed detection, multicast.**

I. Introduction

Spatial division multiple access (SDMA) exploits the multiple antennas at the communication terminals to serve multiple users simultaneously [1]. Utilizing the same time and frequency dimensions, interference is one of the crucial factors that hampers its implementation. Multiple antennas concept introduces spatial degrees of freedom providing the separation of users and limiting the harmful effects of interference thereby allowing spatial multiplexing [1]- [9].

The applications of SDMA, in which a transmitter equipped with multiple antennas aims to communicate with multiple receivers, vary according to the requested service. The first service type is known as a broadcast in which a transmitter has a common message to be sent to multiple receivers. In physical layer research, this service has been studied under the term of physical layer multicasting (i.e. *PHY multicasting*) [14]- [15]. Since a single data stream is sent to all receivers, there is no multiuser interference. In the remainder of this paper, this case will be referred to as multicast transmission. The second service type is known as unicast, in which a transmitter has an individual message for each receiver. Due to the nature of the wireless medium and the use of multiple antennas, multiple simultaneous unicast transmissions are possible in the downlink of a base station (BS). In these cases, multiple streams are simultaneously sent, which motivates precoding techniques that mitigate the multiuser interference. In information theory terms, this service type has been studied using the broadcast channel [9]. In the remainder of this paper, this case will be referred to as *downlink* transmission.

In the literature, the precoding techniques for downlink transmissions can be further classified as [27]:

1) *Group-level precoding* in which multiple codewords are transmitted simultaneously but each codeword is addressed to a group of users. This case is also known as multigroup multicast precoding [18]- [21] and the precoder design is dependent on the channels in each user group.
2) *User-level precoding* in which multiple codewords are transmitted simultaneously but each codeword is addressed to a single user. This case is also known as multiantenna broadcast channel precoding [6]- [13] and the precoder design depends on the channels of the individual users. This is a special case of group level precoding where each group consists of a single user.
3) *Symbol-level precoding* in which multiple symbols are transmitted simultaneously and each symbol is addressed to a single user [22]- [27]. This is also known as a constructive interference precoding and the precoder design is dependent on both the channels (CSI) and the symbols of the users (DI).

The main idea of symbol-based precoding is to jointly utilize the spatial cross-coupling between the users' channel and the received symbols which depend on both channel state and transmitted symbols. When untreated, this cross-coupling leads to interference among the symbol streams of the users. Several spatial processing techniques decouple the multiuser transmission to reduce the interference power received at each terminal [9]. On the other hand, [22] classifies the

Maha Alodeh, Symeon Chantzinotas and Björn Ottersten are with Interdisciplinary Centre for Security Reliability and Trust (SnT) at the University of Luxembourg, Luxembourg. E-mails:{ maha.alodeh@uni.lu, symeon.chatzinotas @uni.lu, and bjorn.ottersten@uni.lu}.
This work is supported by Fond National de la Recherche Luxembourg (FNR) projects, project Smart Resource Allocation for Satellite Cognitive Radio (SRAT-SCR) ID:4919957 and Spectrum Management and Interference Mitigation in Cognitive Radio Satellite Networks SeMiGod.

interference in the scenario of BPSK and QPSK into two types: constructive and destructive. Based on this classification, a selective channel inversion scheme is proposed to cancel the destructive interference while retaining the constructive one to be received at the users' terminal. A more elaborated scheme is proposed in [23], which rotates the destructive interference to be received as useful signal with the constructive one. Moreover, exploiting the interference within Tomlinson and Harashima precoding (THP) has been investigated in [24], this requires an additional complexity due to modulo operation at the receiver side. These schemes outperform the conventional precoding schemes [9] and show considerable gains. However, the anticipated gains come at the expense of additional complexity at the system design level. Assuming that the channel coherence time is τ_c, and the symbol period is τ_s, with $\tau_c \gg \tau_s$ for slow fading channels, the user precoder has to be recalculated with a frequency of $\frac{1}{\tau_c}$ in comparison with the symbol based precoder $\frac{1}{\min(\tau_c,\tau_s)} = \frac{1}{\tau_s} = f_s$. In the symbol-level precoding, the number of possible calculations depends on the number of the users and the adopted modulation. Assuming that frame has L symbols, the number of the possible calculations equals to $\min\{L, 2^{\sum_j m_j}\}$, where m_j is the modulation order for the j^{th} user. Therefore, faster precoder calculation and switching is needed in the symbol-level precoding which can be translated to more complex and expensive hardware.

In this direction, [26]- [27] have proposed a symbol based precoding to exploit the interference by establishing the connection between the constructive interference precoding and PHY- multicasting. Moreover, several constructive interference precoding schemes have been proposed in [27], including Maximum ratio transmission (MRT)-based algorithm and objective-driven constructive interference techniques. The MRT based algorithm, titled as Constructive interference MRT (CIMRT), exploits the singular value decomposition (SVD) of the concatenated channel matrix. This enables the decoupled rotation using Givens rotation matrices between the users' channels subspaces to ensure that the interference is received constructively at the users. On the other hand, the objective-driven optimization formulates the constructive interference problem by considering its relation to PHY-multicasting. Many metrics are addressed such as minimizing transmit power, maximizing the minimum SNR and maximizing the sum rate. However, the aforementioned precoding techniques design the transmitted signal so that it is received exactly the desired constellation point. Based on this novel approach, authors in [29] have extended the multicast-based symbol-level precoding for imperfect CSI by proposing a robust precoding scheme.

In the current paper, we aim at optimizing the constructive interference among the spatial streams while we allow for more flexible precoding design. We exploit the fact that the received symbol should lie in the correct detection region but not necessarily at the exact constellation point. This provides flexibility at the precoding design level in comparison with [26]- [27], where the precoding is designed to target the exact constellation point (see Fig. 1). Rather than designing the sum of interfering and target signals to point at the target constellation point, we relax this condition by allowing it to refer to any point that lies inside a predefined phase margin within the detection region. Therefore, the received signal can be detected correctly at the user's terminal. As shown herein, this flexibility can be translated into more energy-efficient transmissions.

The contribution of the paper can be summarized as:

- Based on the constructive interference definition [27] and the relaxed detection region concept, we propose a symbol level precoding that minimizes the transmit power subject to SNR target constraints and maximizes the minimum SNR subject to total transmit power.
- The impact of relaxed detection on the symbol error rate and consequently the effective rate is analyzed.
- The trade off between SER increase (effective rate) and the transmit power saving is investigated by exploiting an energy efficiency metric.

The single amplitude modulation (e.g. MPSK) can be exploited in communication systems due to their optimality in wideband communications [30], which motivates their usage in low data rate and satellite communications [31]. Moreover, the lower-order modulations (BPSK, QPSK) are used to ensure a reliable communication process at low SINR scenario. Furthermore, they can be exploited in large scale MIMO systems [32].

The rest of the paper is organized as follows: the channel and system model are explained in section (II), while section (III) revisits the definition of constructive interference. Section (IV) exploits the constructive interference with relaxed detection in symbol-level precoding that minimizes the transmit power subject to SNR target. Moreover, the problem of maximizing the minimum SINR is tackled in section (V). The symbol error rate performance is studied in section (VI). The impact of the increased error resulting from relaxed detection region on the effective rate is discussed by studying the energy efficiency metric in section (VII). Finally, the performance of the proposed algorithms is evaluated in section (VIII).

Notation: We use boldface upper and lower case letters for matrices and column vectors, respectively. $(\cdot)^H$, $(\cdot)^*$ stand for Hermitian transpose and conjugate of $(\cdot)$. $\mathbb{E}(\cdot)$ and $\|\cdot\|$ denote the statistical expectation and the Euclidean norm, $\mathbf{A} \succeq \mathbf{0}$ is used to indicate the positive semidefinite matrix. $\angle(\cdot)$, $|\cdot|$ are the angle and magnitude of $(\cdot)$ respectively. $\mathcal{R}(\cdot)$, $\mathcal{I}(\cdot)$ are the real and the imaginary part of $(\cdot)$, i indicates the complex part of the number. Finally, the vector of all zeros with length of K is defined as $\mathbf{0}^{K\times 1}$.

II. System and Signal Models

We consider a single-cell multiple-antenna downlink scenario, where a single BS is equipped with M transmit antennas that serves K user terminals, each one of them equipped with a single receiving antenna. The adopted modulation technique is M-PSK. We assume a quasi static block fading channel $\mathbf{h}_j \in \mathbb{C}^{1\times M}$ between the BS antennas and the j^{th} user, where the received signal at j^{th} user is written as

$$y_j[n] \quad = \quad \mathbf{h}_j\mathbf{x}[n] + z_j[n]. \tag{1}$$

$\mathbf{x}[n] \in \mathbb{C}^{M\times 1}$ is the transmitted symbol sampled signal vector at time n from the multiple antennas transmitter and z_j denotes the noise at j^{th} receiver, which is assumed i.d.d complex Gaussian distributed variable $\mathcal{CN}(0,\sigma_n^2)$. A compact formulation of the received signal at all users' receivers can be written as

$$\mathbf{y}[n] \quad = \quad \mathbf{H}\mathbf{x}[n] + \mathbf{z}[n]. \tag{2}$$

Let $\mathbf{x}[n]$ be written as $\mathbf{x}[n] = \sum_{j=1}^{K} \sqrt{p_j[n]}\mathbf{w}_j[n]d_j[n]$, where $\mathbf{w}_j$ is the $\mathbb{C}^{M\times 1}$ unit power precoding vector for the user j. The received signal at j^{th} user y_j in n^{th} symbol period is given by

$$y_j[n] = \sqrt{p_j[n]}\mathbf{h}_j\mathbf{w}_j[n]d_j[n] + \sum_{k\neq j}\sqrt{p_k[n]}\mathbf{h}_j\mathbf{w}_k[n]d_k[n] + z_j[n] \tag{3}$$

where p_j is the allocated power to the j^{th} user. A more detailed compact system formulation is obtained by stacking the received signals and the noise components for the set of K selected users as

$$\mathbf{y}[n] = \mathbf{H}\mathbf{W}[n]\mathbf{P}^{\frac{1}{2}}[n]\mathbf{d}[n] + \mathbf{z}[n] \tag{4}$$

with $\mathbf{H} = [\mathbf{h}_1,\ldots,\mathbf{h}_K]^T \in \mathbb{C}^{K\times M}$, $\mathbf{W} = [\mathbf{w}_1,\ldots,\mathbf{w}_K] \in \mathbb{C}^{nt\times M}$ as the compact channel and precoding matrices. Notice that the transmitted signal $\mathbf{d} \in \mathbb{C}^{K\times 1}$ includes the uncorrelated data symbols d_k for all users with $\mathbb{E}[|d_k|^2] = 1$, $\mathbf{P}^{\frac{1}{2}}[n]$ is the power allocation matrix $\mathbf{P}^{\frac{1}{2}}[n] = diag(\sqrt{p_1[n]},\ldots,\sqrt{p_K[n]})$. It should be noted that both CSI and data information (DI) are available at the transmitter side. From now on, we assume that the precoding design is performed at each symbol period and accordingly we drop the time index for the sake of notation.

A. Power constraint

In the conventional user-level precoding, the transmitter needs to precode every τ_c which means that the power constraint has to be satisfied along the coherence time $\mathbb{E}_{\tau_c}\{\|\mathbf{x}\|^2\} \leq P$. Taking the expectation of $\mathbb{E}_{\tau_c}\{\|\mathbf{x}\|^2\} = \mathbb{E}_{\tau_c}\{tr(\mathbf{W}\mathbf{d}\mathbf{d}^H\mathbf{W}^H)\}$, and since $\mathbf{W}$ is fixed along τ_c, the previous expression can be reformulated as $tr(\mathbf{W}\mathbb{E}_{\tau_c}\{\mathbf{d}\mathbf{d}^H\}\mathbf{W}^H) = tr(\mathbf{W}\mathbf{W}^H) = \sum_{j=1}^{K}\|\mathbf{w}_j\|^2$, where $\mathbb{E}_{\tau_c}\{\mathbf{d}\mathbf{d}^H\} = \mathbf{I}$ due to uncorrelated symbols over τ_c.

However, in symbol level precoding the power constraint should be guaranteed for each symbol vector transmission namely for each τ_s. In this case the power constraint equals to $\|\mathbf{x}\|^2 = \mathbf{W}\mathbf{d}\mathbf{d}^H\mathbf{W}^H = \|\sum_{j=1}^{K}\mathbf{w}_j d_j\|^2$. In the next sections, we characterize the constructive interference and show how to exploit it in the multiuser downlink transmissions.

III. Constructive Interference

In the symbol level precoding for MPSK modulation, interference can be constructed in advance in order to push the received symbols further into the correct detection region and, as a consequence it enhances the system performance. Therefore, the interference can be classified into constructive or destructive based on whether it facilitates or deteriorates the correct detection of the received symbol. For BPSK and QPSK scenarios, a detailed classification of interference is discussed thoroughly in [22]. The required conditions to have constructive interference for any M-PSK modulation have been described in [27], but we mention here the definition of constructive interference for the sake of completeness.

A. Constructive Interference Definition

Assuming both DI and CSI are available at the transmitter, the unit-power created interference from the k^{th} data stream on j^{th} user can be formulated as:

$$\rho_{jk} = \frac{\mathbf{h}_j\mathbf{w}_k}{\|\mathbf{h}_j\|\|\mathbf{w}_k\|}. \tag{5}$$

Since the adopted modulations are M-PSK ones, a definition for constructive interference can be stated as:

Lemma [27]. *An M-PSK modulated symbol d_k is said to receive constructive interference from another simultaneously transmitted symbol d_j which is associated with $\mathbf{w}_j$ if and only if the following inequalities hold*

$$\angle d_j - \frac{\pi}{M} \leq \arctan\left(\frac{\mathcal{I}\{\rho_{jk}d_k\}}{\mathcal{R}\{\rho_{jk}d_k\}}\right) \leq \angle d_j + \frac{\pi}{M},$$

$$\mathcal{R}\{d_k\}.\mathcal{R}\{\rho_{jk}d_j\} > 0, \mathcal{I}\{d_k\}.\mathcal{I}\{\rho_{jk}d_j\} > 0.$$

It should be noted that the constructive interference is mutual. If the symbol d_j constructively interferes with d_k, then the interference from transmitting the symbol d_k is constructive to d_j [27].

IV. Constructive Interference for Power Minimization

A. Constructive Interference Power Minimization Precoding (CIPM) with Strict Constellation Targets [27]

From the definition of constructive interference, we should design the constructive interference precoders by granting that the sum of the precoders and data symbols forces the received signal to an exact MPSK constellation point namely an exact phase for each user. Therefore, the optimization that minimizes the transmit power and guarantees the constructive reception of the transmitted data symbols can be written as

$$\begin{aligned}\mathbf{w}_k(d_j,\mathbf{H},\boldsymbol{\zeta}) \;&= \arg\min_{\mathbf{w}_1,\ldots,\mathbf{w}_K} \quad \|\sum_{k=1}^{K}\mathbf{w}_k d_k\|^2 \\ s.t. \quad &\begin{cases}\mathcal{C}1: \angle(\mathbf{h}_j\sum_{k=1}^{K}\mathbf{w}_k d_k) = \angle(d_j), \forall j\in K \\ \mathcal{C}2: \|\mathbf{h}_j\sum_{k=1}^{K}\mathbf{w}_k d_k\|^2 \geq \sigma_n^2\zeta_j \quad ,\forall j\in K,\end{cases}\end{aligned} \tag{6}$$

where ζ_j is the SNR target for the j^{th} user, and $\boldsymbol{\zeta} = [\zeta_1,\ldots,\zeta_K]$ is the vector that contains all the SNR targets. The set of constraints $\mathcal{C}_1$ guarantees that the received signal for each user has the correct phase so that the right MPSK symbol d_j can be detected.

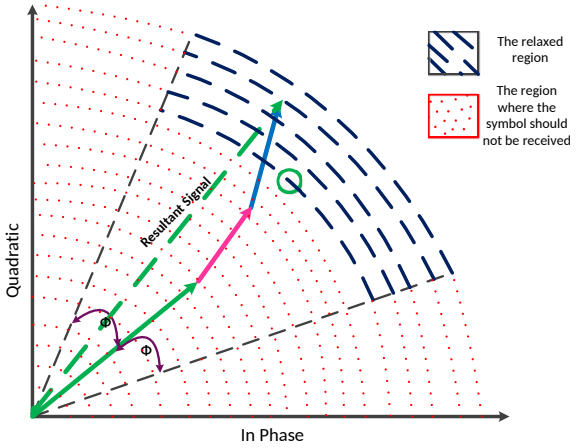

Fig. 1. Constructive Interference Symbol Level Precoding in Multiuser MISO Based on Relaxed Detection Region. The phase ϕ delimits the relaxed region.

B. Proposed Constructive Interference Power Minimization precoding with Relaxed Detection Region

To grant a correct M-PSK symbol detection, the received symbol should lie in the correct detection region. Fig. (1) depicts the detection region of the QPSK symbol $\frac{1+i}{\sqrt{2}}$ which spans the phases $[0°, 90°]$. In the previous section, we designed the transmitted symbol to be received with the exact phase of the target data symbols except the random deviation resulting from the noise at the receiver. On the other hand, the same symbol can be correctly detected as "11" within a range of phases as long as it lies in the first quadrant and the receiver noise does not push it outside the detection region. Therefore, it is not necessary to design precoding so that it aims the exact phase, but the targeted receive symbol can span the range of $[45-\phi, 45+\phi]$ with $0 \leq \phi \leq 45$, where ϕ denotes the phase margin of the relaxed detection region. Therefore, more flexibility for the system design can be obtained and higher gains can be harnessed as shown in the numerical results section. It should be noted that the above example is for QPSK, but the concept is straightforwardly extendable to other MPSK modulations. Since the detection region of symbols span different phases, we can utilize this property by relaxing the transmitted constellation point to include this angular span, which is called the *relaxed detection region*. The relaxed optimization can be formulated as

$$\mathbf{w}_j(\mathbf{H},\mathbf{d},\boldsymbol{\zeta},\boldsymbol{\Phi}_1,\boldsymbol{\Phi}_2) = \arg\min_{\mathbf{w}_j} \quad \|\sum_{j=1}^{K}\mathbf{w}_j d_j\|^2$$
$$s.t. \quad \begin{cases} \mathcal{C}_1 : \angle(\underbrace{d_j-\phi_{j1}}_{\phi'_{j1}}) \leq \angle(\mathbf{h}_j\sum_{j=1}^{K}\mathbf{w}_j) \leq \angle(\underbrace{d_j+\phi_{j2}}_{\phi'_{j2}}), \forall j \in K \\ \mathcal{C}_2 : \|\mathbf{h}_j\sum_{j=1}^{K}\mathbf{w}_j\|^2 \geq \sigma_n^2\zeta_j \quad \forall j \in K. \end{cases}$$

If we use $\mathbf{x} = \sum_{j=1}\mathbf{w}_j d_j$, the problem can be expressed as

$$\mathbf{x} \quad (\mathbf{H},\mathbf{d},\boldsymbol{\zeta},\boldsymbol{\Phi}_1,\boldsymbol{\Phi}_2) = \arg\min_{\mathbf{x}} \quad \|\mathbf{x}\|^2$$
$$s.t. \quad \begin{cases} \mathcal{C}_1 : \angle(\underbrace{d_j-\phi_{j1}}_{\phi'_{j1}}) \leq \angle(\mathbf{h}_j\mathbf{x}) \leq \angle(\underbrace{d_j+\phi_{j2}}_{\phi'_{j2}}), \forall j \in K \\ \mathcal{C}_2 : \|\mathbf{h}_j\mathbf{x}\|^2 \geq \sigma_n^2\zeta_j \quad \forall j \in K. \end{cases}$$

where ϕ_{j1} and ϕ_{j2} are the phase thresholds that received symbols should lie in without the noise drifting, $\boldsymbol{\phi}_1$ and $\boldsymbol{\phi}_2$ are the vectors that contain all ϕ_{j1} and ϕ_{j2} respectively. Although this relaxes the phase constraints on the constructive interference design, it increases the system susceptibility to noise. Therefore, this phase margin should be related to the SNR targets to guarantee certain power saving and SER by selecting the allowable values of ϕ_{j1} and ϕ_{j2}. The optimization can be written[1]

$$\mathbf{x} \quad (\mathbf{H},\mathbf{d},\boldsymbol{\zeta},\boldsymbol{\Phi}_1,\boldsymbol{\Phi}_2) = \arg\min_{\mathbf{x}} \quad \|\mathbf{x}\|^2 \tag{8}$$
$$s.t. \quad \begin{cases} \mathcal{C}_1 : \mathbf{h}_j\mathbf{x} + \mathbf{x}^H\mathbf{h}_j^H \gtrless 2\sigma_n\sqrt{\zeta_j}u_j, \forall j \in K \\ \mathcal{C}_2 : \mathbf{h}_j\mathbf{x} - \mathbf{x}^H\mathbf{h}_j^H \gtrless \pm 2i\sigma_n\sqrt{\zeta_j}\sqrt{1-u_j^2}, \forall j \in K \\ \mathcal{C}_3 : \cos(\phi'_{j2}) \leq u_j \leq \cos(\phi'_{j1}), \forall j \in K \end{cases}$$

where u_j is an auxiliary variable. This optimization has $3K$ constraints that need to be satisfied. The Lagrangian for this problem can be written as

$$\begin{aligned} \mathcal{L}(\mathbf{x}) &= \|\mathbf{x}\|^2 + \sum_j \alpha_j(\mathbf{h}_j\mathbf{x} + \mathbf{x}^H\mathbf{h}_j^H - 2\sigma_n\sqrt{\zeta_j}u_j) \\ &+ \sum_j \mu_j(\mathbf{h}_j\mathbf{x} - \mathbf{x}^H\mathbf{h}_j^H - 2i\sigma_n\sqrt{\zeta_j}\sqrt{1-u_j^2}) \\ &+ \sum_j \lambda_j(u_j - \cos(\phi'_{j,1}))) + \sum_j \gamma_j(u_j - \cos(\phi'_{j,2}))). \end{aligned}$$

[1] $\pm$ in ($\mathcal{C}_2$-8) indicates that the sign can be positive or negative depending on the value of $\sin\phi$ function

Differentiating $\mathcal{L}(\mathbf{x})$ with respect to $\mathbf{x}^*$ and u_j yields:

$$\begin{aligned}\frac{\partial \mathcal{L}(\mathbf{x},u_j)}{\partial \mathbf{x}} &= \mathbf{x}+\sum_j \alpha_j \mathbf{h}_j^H - \sum_j \mu_j \mathbf{h}_j^H, \\ \frac{\partial \mathcal{L}(\mathbf{x},u_j)}{\partial u_j} &= -2\sigma_n\sqrt{\zeta_j}+2i\sigma_n\sqrt{\zeta_j}\frac{u_i}{\sqrt{1-u_i^2}}+\lambda_j+\gamma_j,\end{aligned} \tag{9}$$

By equating $\frac{d\mathcal{L}(\mathbf{x},u_i)}{d\mathbf{x}^*}=0$ and $\frac{d\mathcal{L}(\mathbf{x},u_i)}{d\mathbf{u}_i}=0$, we can get the following expressions

$$\mathbf{x}=\sum_j -\alpha_j \mathbf{h}_j^H+\mu_j \mathbf{h}_j^H \tag{10}$$

$$u_j=\pm\frac{2\sqrt{\zeta_j}-\lambda_j-\gamma_j}{\sqrt{-4\sqrt{\zeta_j}(\lambda_j+\gamma_j)+\lambda_j^2+2\lambda_j\gamma_j+\gamma_j^2}}. \tag{11}$$

Substituting (10)-(11) in the constraints, we have the set of inequalities (12). It can be noted that the solution of (6) is a special case of (13) when ϕ_{j1} and ϕ_{j2} are equal to zero.

1) Equal phase margin solution for power minimization: A simpler solution can be found for the scenario of $\phi_{j1}=\phi_1, \forall j \in K$ and $\phi_{j2}=\phi_2, \forall j \in K$ and $\phi=\phi_1=\phi_2$ by searching all the phases that lie in the relaxed region. The linear search is performed on the value of ϕ_u which is varied from $\angle d_j-\phi_1$ to $\angle d_j+\phi_2$ to achieve the minimum power consumption. For each value $\phi_u \in [\angle d_j-\phi, \angle d_j+\phi]$, we solve the following optimization

$$\begin{aligned}\mathbf{x} \quad & (\mathbf{H},\mathbf{d},\boldsymbol{\zeta},\phi_u)=\arg\min_{\mathbf{x}} \quad \|\mathbf{x}\|^2 \\ s.t. \quad & \begin{cases}\mathcal{C}_1: \mathbf{h}_j\mathbf{x}+\mathbf{x}^H\mathbf{h}_j^H \gtrless 2\sigma_n\sqrt{\zeta_j}\cos(\phi_u), \forall j\in K \\ \mathcal{C}_2: \mathbf{h}_j\mathbf{x}-\mathbf{x}^H\mathbf{h}_j^H \gtrless 2i\sigma_n\sqrt{\zeta_j}\sin(\phi_u), \forall j\in K,\end{cases}\end{aligned} \tag{13}$$

To find the phase within the phase margin that has the minimum power consumption

$$\phi^*=\underset{\phi_u}{\operatorname{argmin}}\|\mathbf{x}(\mathbf{H},\mathbf{d},\boldsymbol{\zeta},\phi_u)\|^2. \tag{14}$$

The relaxed detection region allows for a larger search space to find the optimal CI precoding that requires minimal power to achieve the target SNR. On the other hand, this transmit power reduction comes at the expense of increasing the symbol error rate (SER) due to the expected noise deviation of the received symbols from their exact constellation, which is analytically studied in section (VI) and numerically in section (VIII).

C. Constructive Interference Power Minimization Bounds

In order to assess the performance of the proposed algorithm, we use two theoretical upper bound as follows [27]:

1) Genie-aided upper-bound: This bound occurs when all multiuser transmissions are constructively interfering by nature and without the need to optimize the output vector. The genie-aided minimum transmit power in the downlink of multiuser MISO system can be found by solving the following optimization as [27]:

$$\begin{aligned}P_{min} \quad &= \quad \arg\min_{p_1,\ldots,p_K} \quad \sum_{k=1}^{K} p_k \\ & s.t. \quad \|\mathbf{g}_k\|^2(|\xi_{kk}|^2 p_k+\sum_{j=1,j\neq k}^{K} p_j|\xi_{kj}|^2)\geq \zeta_k\sigma_n^2, \forall k\in K.\end{aligned} \tag{15}$$

If we assume $\mathbf{W}=\mathbf{H}^{'}$, where $\mathbf{H}^{'}=[\frac{\mathbf{h}_1^H}{\|\mathbf{h}_1\|},\ldots,\frac{\mathbf{h}_K^H}{\|\mathbf{h}_K\|}]$. By exploiting singular value decomposition (SVD) of $\mathbf{H}=\mathbf{S}\mathbf{V}\mathbf{D}^H$ and $\mathbf{W}=\mathbf{D}\mathbf{V}^{'}\mathbf{S}^H$, where $\mathbf{V}$,$\mathbf{V}^{'}$ are diagonal matrices that contain the singular values of $\mathbf{H}$ and $\mathbf{W}$. The received signal can be expressed as

$$\mathbf{y} \quad = \quad \mathbf{H}\mathbf{W}\mathbf{d}=\mathbf{S}\mathbf{V}\mathbf{D}\mathbf{D}^H\mathbf{V}^{'}\mathbf{S}^H\mathbf{P}^{1/2}\mathbf{d}. \tag{16}$$

If we denote $\mathbf{G}=\mathbf{S}\mathbf{V}\mathbf{D}\mathbf{D}^H$ and $\mathbf{B}=\mathbf{S}^H$. Utilizing the reformulation of $\mathbf{y}$ in (16), the received signal can be written as

$$y_j=\|\mathbf{g}_j\|\sum_{k=1}^{K}\sqrt{p_k}\xi_{jk}d_k, \tag{17}$$

where $\mathbf{g}_j$ is the j^{th} row of the matrix $\mathbf{G}$, $\xi_{jk}=\frac{\mathbf{g}_j\mathbf{b}_k}{\|\mathbf{g}_j\|}$.

2) Optimal Multicast: The relation between Phy-layer multicasting and constructive interference is proven in [27]. The optimal input covariance $\mathbf{Q}$ for power minimization in a multicast system can be found as a solution of the following optimization

$$\min_{\mathbf{Q}:\mathbf{Q}\succeq 0} \quad tr(\mathbf{Q}) \quad s.t. \quad \mathbf{h}_j\mathbf{Q}\mathbf{h}_j^H\geq\sigma_n^2\zeta_j \quad ,\forall j\in K \tag{18}$$

This problem is thoroughly solved in [14].

V. Weighted Max-Min SINR Algorithm for Constructive Interference Precoding (CIMM) Based on Relaxed Detection

The weighted max-min SINR precoding enhances the relative fairness in the system by maximizing the worst user SINR. This problem has been discussed in various scenarios such as multiuser downlink transmissions [10], and multicast [14]. The authors of [10] have solved the problem using the bisection technique. On the other hand, the authors in [14] have tackled this problem by finding the relation between the min-power problem and max-min problem and formulating both problem as convex optimization ones. [27] utilize the constructive interference to enhance the fairness in terms of weighted SNR. The challenging aspects are the additional constraints which guarantee that the data have been detected correctly at the receivers. The constructive interference max-min problem with strict phase constraints can be formulated as [27]:

$$
\begin{array}{lcl}
0.5\|\mathbf{h}_1\|(\sum_k(-\mu_k+\alpha_k i)\|\mathbf{h}_k\|\rho_{1k} & - & \sum_k(-\mu_k+\alpha_k i)\|\mathbf{h}_k\|\rho^*_{1k}) = \sqrt{\zeta_1}\sqrt{1-\frac{(2\sqrt{\zeta_1}-\lambda_1-\gamma_1)^2}{-4\sqrt{\zeta_1}(\lambda_1+\gamma_1)+\lambda_1^2+2\lambda_1\gamma_1+\gamma_1^2}} \\
0.5\|\mathbf{h}_1\|(\sum_k(-\mu_k i-\alpha_k)\|\mathbf{h}_k\|\rho_{1k} & + & \sum_k(-\mu_k i-\alpha_k)\|\mathbf{h}_k\|\rho^*_{1k}) = \sqrt{\zeta_1}\frac{2\sqrt{\zeta_1}-\lambda_1-\gamma_1}{\sqrt{-4\sqrt{\zeta_1}(\lambda_1+\gamma_1)+\lambda_1^2+2\lambda_1\gamma_1+\gamma_1^2}} \\
 & \vdots & \\
0.5\|\mathbf{h}_K\|(\sum_k(-\mu_k+\alpha_k i)\|\mathbf{h}_k\|\rho_{Kk} & - & \sum_k(-\mu_k+\alpha_k i)\|\mathbf{h}_k\|\rho^*_{Kk}) = \sqrt{\zeta_K}\sqrt{1-\frac{(2\sqrt{\zeta_K}-\lambda_K-\gamma_K)^2}{-4\sqrt{\zeta_K}(\lambda_K+\gamma_K)+\lambda_K^2+2\lambda_K\gamma_K+\gamma_K^2}} \\
0.5\|\mathbf{h}_K\|(\sum_k(-\mu_k i-\alpha_k)\|\mathbf{h}_k\|\rho_{Kk} & + & \sum_k(-\mu_k i-\alpha_k)\|\mathbf{h}_k\|\rho^*_{Kk}) = \sqrt{\zeta_K}\frac{2\sqrt{\zeta_K}-\lambda_K-\gamma_K}{\sqrt{-4\sqrt{\zeta_K}(\lambda_K+\gamma_K)+\lambda_K^2+2\lambda_K\gamma_K+\gamma_K^2}} \\
2\sqrt{\zeta_1}-\lambda_1-\gamma_1 & \leq & \sqrt{-4\sqrt{\zeta_1}(\lambda_1+\gamma_1)+\lambda_1^2+2\lambda_1\gamma_1+\gamma_1^2}\cos(\phi^{'}_{11}) \\
2\sqrt{\zeta_1}-\lambda_1-\gamma_1 & \geq & \sqrt{-4\sqrt{\zeta_1}(\lambda_1+\gamma_1)+\lambda_1^2+2\lambda_1\gamma_1+\gamma_1^2}\cos(\phi^{'}_{12}) \\
 & \vdots & \\
2\sqrt{\zeta_K}-\lambda_K-\gamma_K & \leq & \sqrt{-4\sqrt{\zeta_K}(\lambda_K+\gamma_K)+\lambda_K^2+2\lambda_K\gamma_K+\gamma_K^2}\cos(\phi^{'}_{K1}) \\
2\sqrt{\zeta_K}-\lambda_K-\gamma_K & \geq & \sqrt{-4\sqrt{\zeta_K}(\lambda_K+\gamma_K)+\lambda_K^2+2\lambda_K\gamma_K+\gamma_K^2}\cos(\phi^{'}_{K2})
\end{array} \tag{12}
$$

$$
\mathbf{w}_k = \max_{\mathbf{w}_k}\min_{j} \quad \left\{\frac{\|\mathbf{h}_j\sum_{k=1}^K \mathbf{w}_k d_k\|^2}{\sigma_n^2 r_j}\right\}_{i=1}^K \tag{19}
$$
$$
s.t. \quad \begin{cases} \mathcal{C}1 : \|\sum_{k=1}^K \mathbf{w}_k d_k\|^2 \leq P \\ \mathcal{C}2 : \angle(\mathbf{h}_j\sum_{k=1}^K \mathbf{w}_k d_k) = \angle(d_j), \quad \forall j \in K. \end{cases}
$$

where r_j denotes the requested SNR target for the j^{th} user and P is the total power that should be allocated to the users. In [14] [27], it has been shown that the optimal output vector is a scaled version of the min-power solution. The weighted max-min SINR problem has been solved using bisection method over $t \in [0,1]$. If we relax the phase constraints of (19), the optimization problem can be formulated as (20). If we denote $\mathbf{x} = \sum_{j=1}^K \mathbf{w}_j d_j$, the optimization problem (20) can be expressed as (21), where $\mathbf{r}$ in (21) denotes the vector that contains all the weights r_j.

A. Equal phase margin solution for max-min SNR

For the scenario of $\phi_{j1} = \phi_1, \forall j \in K$, $\phi_{j2} = \phi_2, \forall j \in K$ and $\phi = \phi_1 = \phi_2$, a simple solution can be found by searching all the phases that lie in the relaxed region. A linear search procedure is performed on the value of ϕ which is varied from $\angle d_j - \phi_1$ to $\angle d_j + \phi_2$ to achieve the objective function. For each value $\phi_u \in [\angle d_j - \phi_1, \angle d_j + \phi_2]$, we solve the following optimization

$$
t(\phi_u) = \arg\max_{t,\phi_u} \quad t \tag{23}
$$
$$
s.t. \quad \begin{cases} \mathcal{C}_1 : \mathbf{h}_j\mathbf{x} + \mathbf{x}^H\mathbf{h}_j^H \gtreqless 2r_j t\cos(\phi_u), \forall j \in K \\ \mathcal{C}_2 : \mathbf{h}_j\mathbf{x} - \mathbf{x}^H\mathbf{h}_j^H \gtreqless 2r_j ti\sin(\phi_u), \forall j \in K, \\ \mathcal{C}_3 : \|\mathbf{x}\|^2 \leq P \end{cases}
$$

to find the phase that achieve the objective function

$$
\phi^* = \operatorname*{argmax}_{\phi_u} \quad t(\phi_u), \tag{24}
$$

where $t(\phi_u)$ is a function that maps the max-min value with its respective phase.

A1: t, ϕ search for max-min SINR for CI precoding (CIMMR)

- Search over $\phi_u \in [\angle d - \phi, \angle d + \phi]$. For each ϕ_u, find
  1) $m_1 \to 0 \qquad m_2 \to 1$
  2) Repeat
  3) set $t_m = \frac{m_1+m_2}{2}$
  4) solve (13) with dropping $\mathcal{C}_3$ and substituting t_m in place of t, set $\hat{P} = \|\mathbf{x}\|^2$
  5) if $\hat{P} \leq P$
     then $t_m \to t_1$
     else $t_m \to t_2$
     Until $|\hat{P} - P| \leq \delta$
  6) $\phi^* = \arg\max t(\phi_u)$
- Return ϕ^*, $t_m(\phi^*)$

B. Complexity of CIPMR and CIMMR

It is hard to assess the complexity of proposed symbol-level precoding as a function of the number of operations since it contains convex optimization problem. The complexity of such optimization depends on the adopted solver. The complexity of CIMM and CIPM are discussed in [27]. CIPMR and CIMMR have additional complexity of $\log_2(N)$, where N is the number of possible values $\frac{\phi_1+\phi_2}{\Delta\phi} = \frac{2\phi}{\Delta\phi}$ and $\Delta\phi$ is the search step size. This additional complexity is due the additional search for the phase ϕ^* that can achieve the minimum transmit power or the highest minimum SNR. In the numerical results section (VIII), we compare the complexity of different algorithms from the run-time perspective.

VI. Symbol Error Rate (SER) Analysis

In this section, we study the SER for symbol-level precoding techniques focusing solely on power minimization problem. It should be noted that the received SNR constraints of the proposed technique eq. (13) are satisfied for each symbol period but not necessarily with equality (as shown in section (VIII), fig.4). However, assuming the symbol based constraint as a lower bound for the average SNR, we formulate the corresponding upper-bound for the SER as a function of the phase margin ϕ. Assuming the SNR constraints are always satisfied by equality, the received signal at the j^{th} user

$$
y_j = (\sqrt{\omega_j}d_j + z_j).
$$

$$\mathbf{w}_k = \max_{\mathbf{w}_k} \min_{j} \quad \left\{ \frac{\|\mathbf{h}_j \sum_{k=1}^{K} \mathbf{w}_k d_k\|^2}{r_j} \right\}_{i=1}^{K} \tag{20}$$
$$s.t. \quad \begin{cases} \mathcal{C}1 : \| \sum_{k=1}^{K} \mathbf{w}_k d_k\|^2 \leq P \\ \mathcal{C}2 : \angle d_j - \phi_{j1} \leq \angle(\mathbf{h}_j \sum_{k=1}^{K} \mathbf{w}_k d_k) \leq \angle(d_j + \phi_{j2}), \quad \forall j \in K. \end{cases}$$

$$\mathbf{x}(\mathbf{H}, \mathbf{d}, \boldsymbol{\zeta}, \boldsymbol{\Phi}_1, \boldsymbol{\Phi}_2, \mathbf{r}) = \max_{\mathbf{x}} \min_{j} \quad \left\{ \frac{\|\mathbf{h}_j \mathbf{x}\|^2}{r_j} \right\}_{i=1}^{K} \tag{21}$$
$$s.t. \quad \begin{cases} \mathcal{C}1 : \|\mathbf{x}\|^2 \leq P \\ \mathcal{C}2 : \angle(d_j - \phi_j) \leq \angle(\mathbf{h}_j \mathbf{x}) \leq \angle(d_j + \phi_{j2}), \quad \forall j \in K \end{cases}$$

$$\max_{t, \mathbf{x}} \quad t \tag{22}$$
$$s.t. \quad \begin{cases} \mathcal{C}1 : \|\mathbf{x}\|^2 \leq P \\ \mathcal{C}2 : \tan(\angle d_j - \phi_{j1}) \leq \frac{\mathbf{h}_j \mathbf{x} - (\mathbf{h}_j \mathbf{x})^H}{i(\mathbf{h}_j \mathbf{x} + (\mathbf{h}_j \mathbf{x})^H)} \leq \tan(\angle d_j + \phi_{j2}), \forall j \in K \\ \mathcal{C}3 : \mathcal{R}\{d_j\}.\mathcal{R}\{\mathbf{h}_j \mathbf{x}\} \geq 0, \forall j \in K \\ \mathcal{C}4 : \mathcal{I}\{d_j\}.\mathcal{I}\{\mathbf{h}_j \mathbf{x}\} \geq 0, \forall j \in K \\ \mathcal{C}5 : \|\mathbf{h}_j \mathbf{x}\|^2 \geq r_j t, \forall j \in K. \end{cases}$$

ω_j is the average received SNR over all symbol realizations at the j^{th} user. In this section, we drop the index for simplicity. By looking at the received signal and taking its projection on the real and imaginary axes, the received signal points can be formulated as

$$\begin{aligned} y &= (r_x, r_y) \\ &= (\sqrt{\omega}\cos(\angle d) + \mathcal{R}\{z\}, \sqrt{\omega}\sin(\angle d) + \mathcal{I}\{z\}) \end{aligned} \tag{25}$$

where r_x, r_y are the projections of the received constellation points on the real and imaginary axes respectively. Since we assume that $\angle d$ and ω are fixed, r_x, r_y take the distribution of the noise which is independent Gaussian. The corresponding probability density function (PDF) of r_x, r_y can be written as

$$\begin{aligned} p(r_x, r_y) &= \frac{1}{\sigma^2 \pi} \exp\left(- \frac{\left(r_x - \sqrt{\omega}\cos(\angle d)\right)^2}{\sigma^2} \right) \\ &\times \exp\left(- \frac{\left(r_y - \sqrt{\omega}\sin(\angle d)\right)^2}{\sigma^2} \right). \end{aligned} \tag{26}$$

If we use the polar coordinate transformation $v = \sqrt{r_x^2 + r_y^2}$, $\theta = \tan(\frac{r_y}{r_x})$, the previous PDF formulation can be written as [38]

$$\begin{aligned} p(v, \theta) = \frac{v}{\pi\sigma^2} &\exp(-\frac{v^2 + \omega + 2\sqrt{\omega} v \cos(\angle d + \theta))}{\sigma^2} \\ &\times \exp(-\frac{2\sqrt{\omega} v \sin(\angle d + \theta)}{\sigma^2}). \end{aligned} \tag{27}$$

For the relaxed detection region design, the SER depends on the angular span ϕ_{j1}, ϕ_{j2}. Intuitively, if we increase this span, the received signal becomes more sensitive to noise. Therefore, the span selection should depend on the value of SNR. We define a new random variable ϕ_j that describes the fact that the transmitted data symbols can be designed to deviate from the central point of the detection region. The value of the ϕ varies according to the target SER. Eq. (26) can be rewritten to include the impact of relaxation as the following

$$\begin{aligned} p(r_1, r_2, \phi) &= \frac{1}{\sigma^2 \pi} \exp\left(- \frac{(r_1 - \sqrt{\omega}\cos(\angle d + \theta + \phi))^2)}{\sigma^2} \right) \\ &\times \exp\left(- \frac{(r_2 - \sqrt{\omega}\sin(\angle d + \theta + \phi))^2}{\sigma^2} \right). \end{aligned} \tag{28}$$

Using the polar coordinates, the PDF that describes the flexible detection region can be expressed as:

$$p(v, \theta, \phi) = \frac{v}{\pi\sigma^2} \exp\Big(- \frac{v^2 + \omega - 2v\sqrt{\omega}\cos(\angle d_k + \theta - \phi)}{\sigma^2} \Big). \tag{29}$$

The SER can be found by formulating the PDF $p(\theta, \phi) = \int_0^\infty p(v, \theta, \phi) dv$

$$\begin{aligned} p(\theta, \phi) = &\exp(-\frac{\sqrt{\omega}\sin(\theta - \phi)}{\sigma^2}) \\ &\times \int_0^\infty v \exp(-\frac{(v - \sqrt{\omega}\cos(\theta - \phi))^2}{\sigma^2}) dv. \end{aligned} \tag{30}$$

The generic formulation for the SER bound for relaxed detection technique can be written as

$$P_e = 1 - \int_{-\frac{\pi}{M}}^{\frac{\pi}{M}} \int_{\angle d - \phi}^{\angle d + \phi} p(\theta, \phi) d\theta d\phi. \tag{31}$$

It should be noted that the formulated SER expression is an upperbound and the actual SER might be larger if the SNR constraints are satisfied by inequality. For CIMM/CIMMR, it is not straightforward to follow the same procedure since the instantaneous SINR changes on symbol basis and we cannot establish a reliable lower-bound for the average SINR in advance.

VII. Trade off analysis

For the relaxed detection design, the transmitted signals are designed to be received with controlled deviation from the exact constellation point to enhance the system performance (i.e. minimize transmit power). The relation between the improvement achieved by allowing such flexibility and the SER performance of the system is studied in this section.

We link the SER analysis with CIPM algorithms (8) in order to find the operating point in terms of phase margin, which minimizes transmit power without considerably degrading the SER. Using (31), the SER considering ζ_k as the minimum acceptable SNR target can be expressed as

$$Pe[\omega_k \geq \zeta_k] = 1 - \int_{-\frac{\pi}{M}}^{\frac{\pi}{M}} \int_{\angle d_j - \phi}^{\angle d_j + \phi} \int_0^{\infty} p(v, \theta, \phi) dv d\phi d\theta.$$

The concept of exploiting the relaxed detection gives the system design more parameters to be tuned and thus more flexibility and performance gain to be anticipated.

A. Effective Rate Analysis

The relaxed detection increases the amount of symbol detection errors, which degrades the rate of each user and affects the performance of whole system. The effective rate for each user can be expressed as

$$\bar{R}_j \approx R_j \times \big(1 - SER(\omega_j, \phi_j)\big) \tag{32}$$

R_j is the target rate of the employed modulation. From (32), it can be concluded that enlarging the relaxed detection region increases the SER and as a result decreases the effective rate in the system.

B. Energy efficiency analysis

The relaxed detection not only decreases the amount of the power required to achieve the target SNR but also decreases the effective rate of the system. To find the optimal balance between these two aspects, the system energy efficiency metric is proposed to find how many bits can be conveyed correctly to the receivers per energy unit[2].The system energy efficiency can be defined as

$$\eta = \frac{\sum_{j=1}^{K} \bar{R}_j \Big(SER_j(\omega_j, \phi_j)\Big)}{P(\Phi, \boldsymbol{\zeta})} \tag{33}$$

where $P(\Phi, \boldsymbol{\zeta}) = \|\mathbf{x}(\mathbf{H}, \mathbf{d}, \boldsymbol{\zeta}, \boldsymbol{\Phi})\|^2$. Assuming equal margin, the optimization can be formulated as

$$\max_{\phi} \quad \eta \tag{34}$$

It should be noted that the energy efficiency is a function of the phase margin since it decreases the transmit power amount required to achieve the target rate. Increasing the phase margin affects both the numerator and the denominator in (33) by decreasing the effective rate and transmit power respectively. Therefore, the impact of the phase margin cannot be straightforwardly deduced. Moreover, it is hard to solve the optimization problem (34) through standard numerical techniques. A simulation-based solution is found in the next section.

[2]The energy efficiency metric is adopted as an assessing metric not as an optimization metric. For further information about energy efficiency optimization, see [36].

Acronym	Technique	equation
1)CIZF	Constructive Interference Zero Forcing	[23]
2)CIMRT	Constructive Interference Maximum Ratio Transmissions	[26]
3)CIPM	Constructive Interference- Power Minimization	6, [27]
4)CIPMR	Constructive interference power minimization with relaxed detection CIPMR[1] $\phi = \frac{\pi}{8}$ CIPMR[2] $\phi = \frac{\pi}{5}$	7
5)CIMM	Constructive interference max min SNR	19, [27]
6)CIMMR	Constructive interference maxmin SNR with relaxed detection region	13,**A**
7)Multicast	Optimal Multicast	18, [14]
8)Genie	Genie theoretical upper-bound	15, [27]
9)OB	Optimal user level beamforming	36, [6]

TABLE I
SUMMARY OF THE PROPOSED (4,6), STATE-OF-THE-ART (1,2,3,5,9) ALGORITHMS AND THE THEORETICAL LOWER BOUND (7,8), THEIR RELATED ACRONYMS, AND THEIR RELATED EQUATIONS AND ALGORITHMS

VIII. Numerical results

In order to assess the performance of the proposed transmissions schemes, Monte-Carlo simulations of the different algorithms have been conducted to study the performance of the proposed techniques and compare to the state of the art techniques. The adopted channel model is assumed to be

$$\mathbf{h}_k \sim \mathcal{CN}(0, \sigma_h^2). \tag{35}$$

σ_h^2 is the channel average power. For the sake of comparison, we use the optimal user-level linear beamforming that aims at minimizing the transmit power which is defined as:

$$\begin{aligned} \mathbf{w}_1, \ldots, \mathbf{w}_K = \quad & \arg\min_{\mathbf{w}_k} \quad \sum_{j=1}^{K} \|\mathbf{w}_k\|^2 \\ & s.t. \quad \frac{\|\mathbf{h}_j \mathbf{w}_j\|^2}{\sum_{k \neq j, k=1}^{K} \|\mathbf{h}_j \mathbf{w}_k\|^2 + \sigma_n^2} \geq \zeta_j \forall j \end{aligned} \tag{36}$$

This problem has been solved in the literature [6].

Fig. (2) depicts the power consumption with respect to target SNR. The comparison among optimal multicast, CIPM and CIPMR is illustrated in this figure while the assumed scenario is $M = 3$, $K = 2$, at $\phi = \frac{\pi}{5}$ and $\frac{\pi}{8}$. It can concluded that the power consumption gap between the optimal multicast and CIPM is fixed for all target rates. This relation holds also for the gap between the CIPMR and CIPM.Moreover, it can be concluded that the CIPMR outperforms CIPM by achieving less power at all target SINR values. Moreover, CIPMR shows a better performance at $\phi = \frac{\pi}{5}$ than $\phi = \frac{\pi}{8}$. Finally, the performance of OB is studied, which presents the optimal user-level precoding that aims at minimizing the transmit power, it can be noted that the symbol level precoding techniques achieves better performance due to the fact that the interference is exploited as an additional energy source.

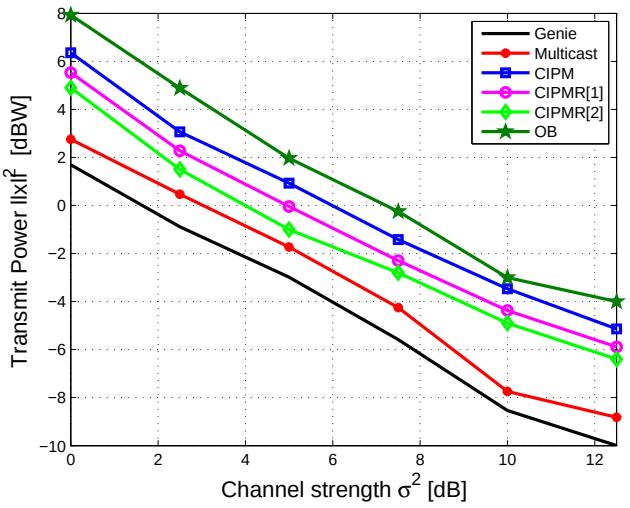

Fig. 2. Transmit power $\|\mathbf{x}\|^2$ vs channel strength σ_h^2. CIPMR[1] denotes the scenario of $\phi = \frac{\pi}{8}$ and CIPMR[2] denotes the scenario of $\phi = \frac{\pi}{5}$.$M = 3$, $K = 2$, $\zeta = 4.7712dB$, QPSK.

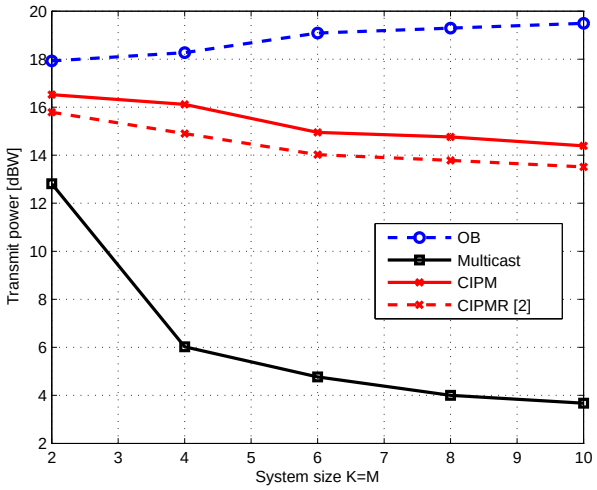

Fig. 3. Transmit power $\|\mathbf{x}\|^2$ vs system size, $\phi = \frac{\pi}{5}$, $\zeta = 6.121dB$, $\sigma_h^2 = 0dB$, QPSK.

Fig. (3) depicts the relation between the transmit power and the system size ($K = M$). It can be noted that by increasing the size of the system, the transmit power using OB increases up to a limit and then it remains almost constant. On the other hand, the transmit power decreases with the system size using multicast, CIPM and CIPMR. CIPM and CIPMR follow this trend with slight difference in the pattern; i.e. multicast tends to have a higher slope in comparison with CIPM and CIPMR.

Fig. (4) depicts the detected signals at users' receivers. The first user should receive "11", which should be detected at the first quadrant. The second user should receive the symbol "00", which should be detected at the third quadrant. The number of the transmitted symbols for each user is "10" symbols. It can be noted that the received signals using CIPMR has higher power than the target SNR. In these cases, the

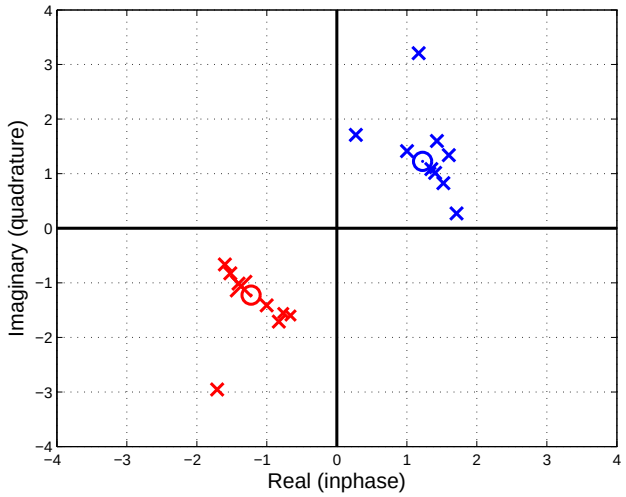

Fig. 4. The received signal using CIPMR and CIPM without the noise effect. $M = 3$, $K = 2$, $\phi = \frac{\pi}{5}$, $\zeta = 4.7121dB$, $\sigma_h^2 = 0dB$, QPSK. The circles denote the detected signal at the receivers assuming CIPM, the crosses denote the detected signal at the receivers assuming CIPMR.

received power at the first user is equal to the target SNR while the other detects its symbol with power higher than its target even though less power is actually used for transmission. This means that the algorithm searches for the phases of the data symbols in the relaxed region that grants the minimum power; sending with certain phase aids the other user and pushes the symbol deeper in the detection region.

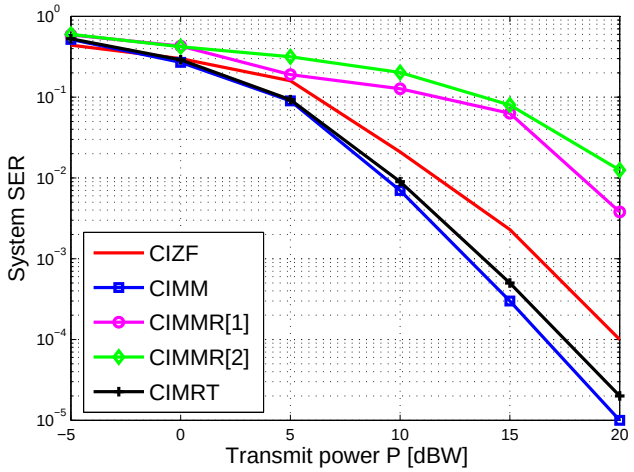

Fig. 5. SER vs transmit power. CIMMR[1] denotes the scenario of $\phi = \frac{\pi}{8}$ and CIMMR[2] denotes the scenario of $\phi = \frac{\pi}{5}$. $M = 3$, $K = 2$, $\sigma_h^2 = 0dB$, QPSK.

The system SER performance with respect to the available power is depicted in Fig.(5). It can be noted that CIMM has the lowest SER. At 20 dB, the SER of CIMM is around 10^{-5} without employing any FEC coding. Moreover, it can be noted that CIMRT has very close performance to CIMM. It also can be deduced that CIZF has a higher SER than CIMM and CIMRT across the studied power range. As expected,

CIMMR has the worst performance in comparison with the other techniques. Varying the angular span of relaxation affects the SER, the SER in the scenario of $\phi = \frac{\pi}{5}$ is close to 10^{-2} at 20 dB, and the SER in the scenario of $\phi = \frac{\pi}{8}$ is around 5×10^{-3}, which is almost half of the value at the scenario of $\phi = \frac{\pi}{8}$.

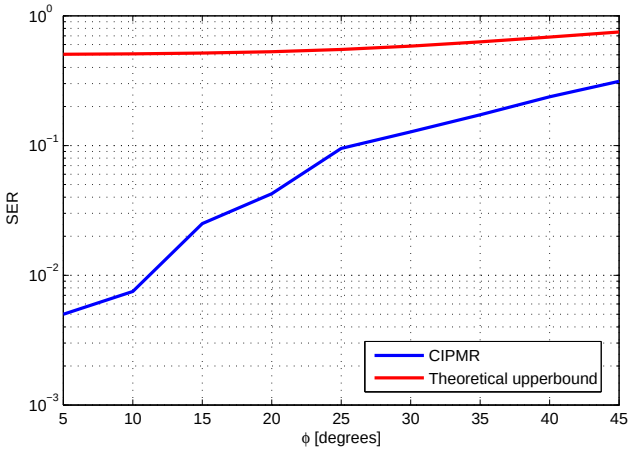

Fig. 6. SER vs angular span ϕ. $M = 3$, $K = 2$, $\sigma^2 = 20dB$, $\zeta = 13db$, $\phi = \frac{\pi}{4}$, QPSK.

Fig. (6) depicts the SER performance of CIPMR with respect to the relaxed phase, SER increases with relaxed phase. Moreover, this figure compares the performance of SER to upperbound in (31).

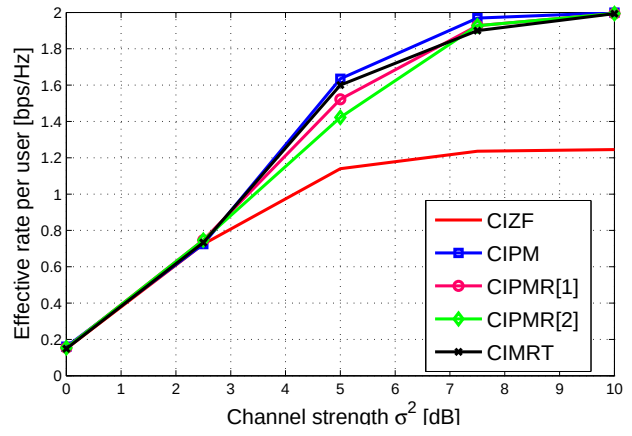

Fig. 7. Rate per user vs. channel strength. CIPMR[1] denotes $\phi = \frac{\pi}{8}$ and CIPMR[2] denotes the scenario of $\frac{\pi}{5}$. $M = 3$, $K = 2$, $\zeta = 4.7121dB$, QPSK.

The effective rate per user versus the channel strength is depicted in Fig. (7). The general trend is that the rate increases with the available power. However, the slope of each curve indicates the amount of rate increase with respect to the available power. Although it has a reasonable SER performance, it can be noted that CIZF has the worst performance from the rate perspective. On the other hand, CIPM achieves the best performance since it has the lowest SER values. CIMRT has a very close performance to CIPM. Regarding the relaxed detection region approach, at $\phi = \frac{\pi}{8}$, the system has a better rate performance than at the scenario $\phi = \frac{\pi}{5}$ due to the higher SER at the latter case. Moreover, all the techniques perform the same at low SNR. In Fig. (8), we depicted the performance

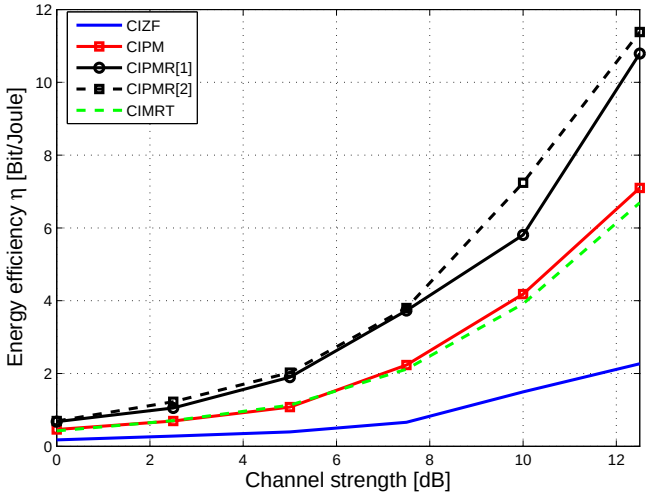

Fig. 8. Energy efficiency η vs channel strength σ_h^2. CIPMR[1] denotes the scenario of $\phi = \frac{\pi}{8}$ and CIMPR[2] denotes the scenario of $\phi = \frac{\pi}{5}$. $M = 3$, $K = 2$, $\sigma^2 = 0dB$, QPSK.

of the proposed techniques from energy efficiency perspective with the channel strength. CIZF shows inferior performance in comparison with all depicted techniques. It has already been proven that CIZF outperforms the conventional techniques like minimum mean square error (MMSE) beamforming and zero forcing beamforming (ZFB) [23]. In comparison with other depicted techniques, it can be concluded that the proposed constructive interference CIPM and CIPMR have better energy efficiency in comparison with CIZF. This can be explained by the channel inversion step in CIZF which wastes energy in decoupling the effective users' channels and before exploiting the interference among the multiuser streams. Moreover, it can be noted that the CIPMR achieves higher energy efficiency than CIPM, since it allows selecting flexibly the target point inside the detection region. Moreover, it can be deduced that CIMRT has a very close performance to CIPM especially at high targets. CIMRT outperforms CIZF at expense of complexity.

Fig. (9) depicts the energy efficiency with respect to SNR targets. We depict the performance of CIZF and CIMRT. For the sake of comparison, the transmit power of the CIZF and CIMRT solutions can be scaled until all users achieve the target rate. It can be noted that CIPMR has a better performance in comparison with the other techniques. The CIPMR has a higher gap at low target SNR values.

Furthermore, the flexibility should be adapted with the target rates. At low target SNR, the flexibility region should be narrowed to prevent from moving outside the correct detection region due to noise. At high target SNR, the flexibility region can be enlarged since the impact of noise can be negligible. This impact is depicted in Fig.(10) at high target SNR.

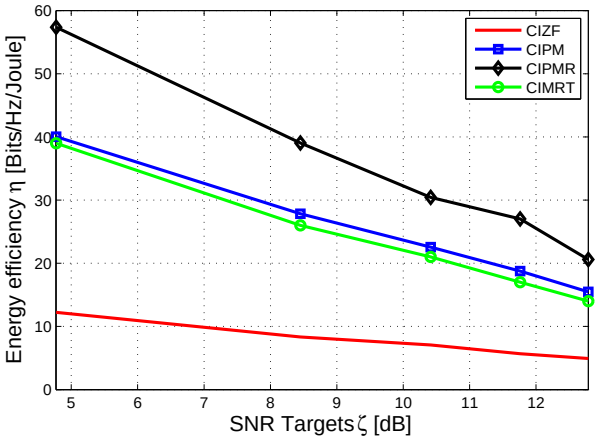

Fig. 9. Energy efficiency η versus SNR targets ζ. $M = 3$, $K = 2$, QPSK, $\sigma_h^2 = 20dB$, $\phi = \frac{\pi}{5}$.

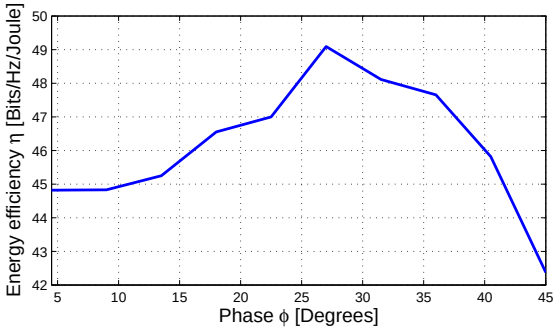

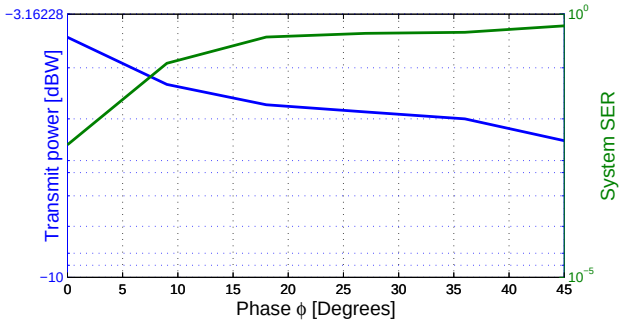

Fig. 10. Energy efficiency, SER, and transmit power vs angular span ϕ. $M = 3$, $k = 2$, QPSK, $\zeta = 13.01dB$, $\sigma_h^2 = 20dB$.

Increasing the angular span of the relaxation decreases the transmit power and increases SER. The two factors influence the energy efficiency of system. Increasing the angular span enhances the energy efficiency to certain limit $\phi = 27°$, and start decreasing gradually, Moreover, it can be noted that SER increases with increasing the angular span. The effect of the flexible angular span at a low SNR target scenario is depicted in fig. (11). It can be noted that the highest energy efficiency is achieved at $\phi = 10°$, which is much lower than the ϕ value that achieves the highest energy efficiency at 20 dB. This means that the impact of the symbol errors overcomes the transmit

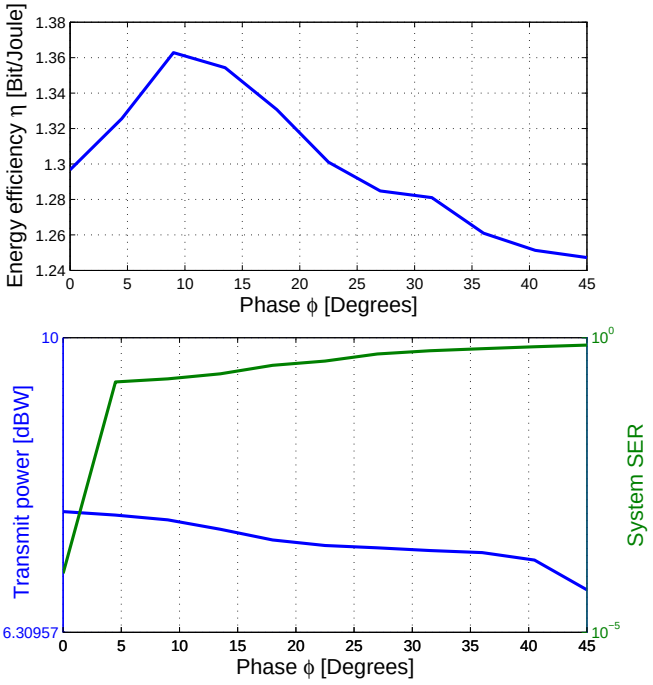

Fig. 11. Energy efficiency, SER and transmit power vs angular span ϕ. $M = 3$, $K = 2$, $\sigma^2 = 0dB$, $\zeta = 4.7712db$, QPSK.

power saving at a much narrower phase margin due to the low SNR. Hence, the result confirms that the optimal phase margin is a function of the SNR targets.

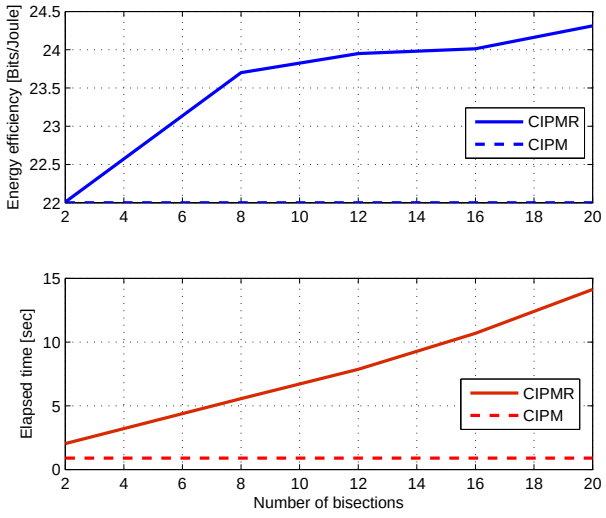

Fig. 12. Energy efficiency and elapsed time vs. number of bisections, $M = 2$, $K = 2$, $\phi = \frac{\pi}{4}$

Fig. (12) depicts the performance of CIPMR with respect to the number of performed bisections to find the optimal phase. The performance is studied from the perspective of energy efficiency and run time simulation to assess the complexity of CIPMR. Since the resolution of the search space improves with the number of bisections, the search time to find the optimal

Mod—ϕ	0	$\frac{\pi}{16}$	$\frac{\pi}{8}$	$\frac{3\pi}{16}$
BPSK	67.75	69.9	71	72.5
QPSK	135.5	139.1	136	121

TABLE II
COMPARISON BETWEEN BPSK AND QPSK FROM ENERGY EFFICIENCY PERSPECTIVE. $M = 3, k = 2, \sigma_h^2 = 20dB, \zeta = 4.712dB$.

Technique/$(M \times K)$	(2× 2)	(3× 3)	(4× 4)	(5× 5)
CIZF	29.4202	21.2105	15.0327	10.4931
CIPM	53.6634	56.3285	65.2014	67.9487
CIPMR	61.5303	88.8655	118.2496	137.8862
Multicast	142.2445	264.6637	389.4930	553.4906

TABLE III
COMPARISON OF THE DIFFERENT TECHNIQUE FROM ENERGY EFFICIENCY PERSPECTIVE PERSPECTIVE. $\sigma_h^2 = 20dB, \zeta = 4.712dB, \phi = \frac{\pi}{5}$, QPSK.

phase increases proportionally with number of bisections. This increases the possibility of finding the peak point of the optimal phase as shown in Fig. (12). Most importantly, the energy efficiency increases with number of bisections, the rate of improvement is high at the low number of bisection and it reduces gradually with the number of the performed bisections. Therefore, a few bisections can provide a large percentage of the performance gain. However, CIPM is independent of bisection, as it does not search for the optimal phase. Fig. (12) illustrates the comparison between CIPM and CIPMR, and it can be concluded that CIPM has lower energy efficiency and lower run-time.

Table (II) illustrates the comparison between QPSK and BPSK modulations in terms of energy efficiency assuming CIPMR. We use the same SNR target for the both modulations. It can be concluded that the energy efficiency increases with the relaxation due to the larger angular span of the BPSK detection region. However, QPSK has a different trend; the energy efficiency increases with the relaxation phase up to a point, and decreases afterwards. This trend is expected to occur at a higher phase in BPSK.

In Table (III), we study the energy efficiency of the different techniques at different (M, K), and full loading $M = K$. It can be concluded that the energy efficiency decreases with system size in CIZF. However, this trend changes in CIPM and CIPMR. It can be noticed that the energy efficiency increases with system size. Moreover, it can be noted that gains achieved by CIPMR is higher than CIPM; for example at (5×5), the energy efficiency of CIPMR is more than twice of CIPM. CIPMR and CIPM follow the same trend of increased energy efficiency with the system size. The complexity of the proposed algorithm is studied in Table (IV) in terms of simulation run-time. We compared the run-time of optimal beamforming (OB) and different symbol-level precoding. From the table, it can be deduced that the run time for OB is the lowest in comparison to the rest. Moreover, the run-time for symbol-level precoding techniques depends on the combinations of the modulation order (possible data symbols) and the number of users, which is explained by the factor κ_x in the table. CIPMR has higher run-time due to the

Technique/$(M \times K)$	(2× 2)	(3× 3)	(4× 4)	(5× 5)
OB	0.2090	0.2512	0.3421	0.3674
CIPM	$0.312 \times \kappa_2$	$0.360 \times \kappa_3$	$0.407 \times \kappa_4$	$0.370 \times \kappa_5$
CIPMR	$9.5 \times \kappa_2$	$9.77 \times \kappa_3$	$10.08 \times \kappa_4$	$10.3 \times \kappa_5$

TABLE IV
COMPARISON OF THE DIFFERENT TECHNIQUE FROM SIMULATION RUN TIME PERSPECTIVE. $\sigma_h^2 = 20dB, \zeta = 4.712dB, \phi = \frac{\pi}{5}$, QPSK, $\kappa_2 = 2^{2\times 2}, \kappa_3 = 2^{3\times 2}, \kappa_4 = 2^{4\times 2}, \kappa_5 = 2^{5\times 2}$.

bisection search, at each iteration, one convex optimization problem is solved, which depends on the solver efficiency. Despite the high complexity of the proposed techniques, it can be argued that with the emerging of cloud RAN, this computational complexity can be transferred to the cloud RAN level [33]. Since the MPSK has limited scalability with respect to SNR, the extension of symbol-level precoding to multi-level modulation (including MQAM) is proposed in [34]- [35].

IX. CONCLUSIONS

In this paper, we design an energy efficient precoding in the downlink of a MU-MISO system. The main idea is based on exploiting the interference among the multiuser transmissions while using symbol-based precoding in combination with MPSK modulations. Particularly, we utilize the concept that the detection region of an M-PSK symbol spans a range of phases, which enables us to relax the system design and to achieve higher power savings. This can be implemented by allowing the precoder to select the optimal phase for each user symbols that can achieve the minimum power without being erroneously detected at the receiver. However, such relaxation increases the system SER. The trade off between the achieved power saving and the SER is characterized by the energy efficiency. The phase margin of the relaxed region can be optimally selected to achieve the highest energy efficiency. The simulation results have confirmed that the relaxed system designs achieve higher energy efficiency especially in the high SNR regime.

REFERENCES

[1] R. H. Roy and B. Ottersten, " Spatial division multiple access wireless communication systems, *US patent*, n° US 5515378A, 1991.

[2] D. Gesbert, M. Kountouris, R. W. Heath Jr., C.-B. Chae and T. Sälzer," From Single User to Multiuser Communications: Shifting the MIMO Paradigm," *IEEE Signal Processing Magazine,* vol. 24 no.5, pp. 36-46, 2007.

[3] Y.-F. Liu, Y.-H. Dai, and Z.-Q. Luo, "Coordinated beamforming for MISO interference channel: Complexity analysis and efficient algorithms,"*IEEE Transactions on Signal Processing*, vol. 59, no. 3, pp. 1142-1157, 2011.

[4] E. Björnson, M. Bengtsson and B. Ottersten, "Optimal Multi-User Transmit Beamforming: Difficult Problem with a Simple Solution Structure," *IEEE Signal Processing Magazine*, 2014.

[5] A. B. Gershman, N. D. Sidiropoulos, S. Shahbazpanahi, M. Bengtsson, and B. Ottersten, "Convex Optimization Based Beamforming," *IEEE Signal Processing Magazine*, vol. 27, no. 3, pp. 62-75, May 2010.

[6] M. Bengtsson and B. Ottersten,"Optimal and Suboptimal Transmit beamforming," in *Handbook of Antennas in Wireless Communications*, L. C. Godara, Ed. CRC Press, 2001.

[7] M. Schubert and H. Boche, "Solution of the Multiuser Downlink Beamforming Problem with Individual SINR Constraints," *IEEE Transaction on Vehicular Technology*, vol. 53, pp. 1828, January 2004.

[8] G. Caire, and S. Shamai (Shitz), "On the Achievable Throughput of a Multiantenna Gaussian Broadcast Channel," *IEEE Transactions on Information Theory*, vol. 49, no. 7, pp. 1691 - 1706, July 2002.

[9] Q. H. Spencer, A.L. Swindlehurst, and M. Haardt, "Zero-forcing Methods for Downlink Spatial Multiplexing in Multiuser MIMO Channels,"*IEEE Transactions on Signal Processing*, vol. 52, no.2, pp. 461-471, February 2004.

[10] A. Wiesel, Y. C. Eldar, and S. Shamai, "Linear precoding via conic optimization for fixed MIMO receivers," *IEEE Transactions on Signal Processing,* vol. 54, no. 1, pp. 161-176, 2006.

[11] Y. Wu, M. Wang, C. Xiao, Z. Ding and X. Gao, "Linear Precoding for MIMO Broadcast Channels with Finite-Alphabets Constraints," *IEEE Transactions on Wireless Communications*, vol. 11, no. 8, pp. 2906-2920, August 2012.

[12] H. Boche, M. Schubert, "Resource allocation in multiantenna systems-achieving max-min fairness by optimizing a sum of inverse SIR," *IEEE Transactions on Signal Processing*, vol. 54 no. 6, pp. 1990-1997, 2006.

[13] R. Ghaffar and R. Knopp, "Near Optimal Linear Precoding for Multiuser MIMO for Discrete Alphabets," *IEEE International Conference on Communications (ICC)*, pp. 1-5, May 2010.

[14] N. D. Sidropoulos, T. N. Davidson, ans Z.-Q. Luo, "Transmit Beamforming for Physical-Layer Multicasting," *IEEE Transactions on Signal Processing*, vol. 54, no. 6, pp. 2239-2251, June 2006.

[15] N. Jindal and Z.-Q. Luo, "Capacity Limits of Multiple Antenna Multicast," *IEEE International Symposium on Information Theory (ISIT)*, pp. 1841 - 1845, June 2006.

[16] B. Du, M. Chen, W. Zhang and C. Pan, "Optimal beamforming for single group multicast systems based on weighted sum rate," *IEEE International Conference on Communications(ICC)*, pp. 4921- 4925, June 2013.

[17] E. Jorswieck, "Beamforming in Interference Networks: Multicast, MISO IFC and Secrecy Capacity," *International Zurich Seminars (IZS)*, March 2011.

[18] E. Karipidis, N. Sidiropoulos and Z.-Q Luo, "Transmit Beamforming to multiple Co-channel Multicast Groups," *IEEE International Workshop on Computational Advances in Multi-Sensor Adaptive Processing (CAMSAP)*, pp. 109-112, December 2005.

[19] D. Christopoulos, S. Chatzinotas and B. Ottersten, "Weighted Fair Multicast Multigroup Beamforming under Per-antenna Power Constraints," *IEEE Transactions on Signal Processing, vol. 62, no. 19, pp. 5132-5142, available arXiv:1406.7557 [cs.IT]*, 2014.

[20] D. Christopoulos, S. Chatzinotas and B. Ottersten, "Full Frequency Reuse Multibeam SatComs: Frame Based Precoding and User Scheduling," *Submitted to IEEE Transactions on Wireless Communications, available arXiv:1406.7699 [cs.IT]*, 2014.

[21] Y. C. B. Silva and A. Klein, "Linear Transmit Beamforming Techniques for the Multigroup Multicast Scenario,"*IEEE Transaction on Vehicular Technology*, vol. 58, no. 8, pp. 4353 - 4367, October 2009.

[22] C. Masouros and E. Alsusa, "Dynamic Linear Precoding for the exploitation of Known Interference in MIMO Broadcast Systems," *IEEE Transactions On Communications*, vol. 8, no. 3, pp. 1396 - 1404, March 2009.

[23] C. Masouros, "Correlation Rotation Linear Precoding for MIMO Broadcast Communications," *IEEE Transactions on Signal Processing*, vol. 59, no. 1, pp. 252 - 262, January 2011.

[24] C. Masouros, M. Sellathurai, T. Ratnarajah,"Interference optimization for transmit power reduction in Tomlinson-Harashima precoded MIMO downlinks," *IEEE Transactions on Signal Processing*, vol. 60 no. 5, pp. 2470-2481, May 2012.

[25] M. Alodeh, S. Chatzinotas and B. Ottersten, "Data Aware User Selection in the Cognitive Downlink MISO Precoding Systems," *invited paper to IEEE International Symposium on Signal Processing and Information Technology (ISSPIT)*, December 2013.

[26] M. Alodeh, S. Chatzinotas and B. Ottersten, "A Multicast Approach for Constructive Interference Precoding in MISO Downlink Channel,"*International Symposium in Information theory (ISIT) 2014, Available on arXiv:1401.6580v2 [cs.IT].*

[27] M. Alodeh, S. Chatzinotas and B. Ottersten, "Constructive Multiuser Interference in Symbol Level Precoding for the MISO Downlink Channel," *IEEE Transactions on Signal processing*, vol. 63, no. 9, pp. 2239-2253, May, 2015, Available on arXiv:1401.4700 [cs.IT].

[28] M. Alodeh, S. Chatzinotas and B. Ottersten, "Energy Efficient Symbol-Level Precoding in Multiuser MISO Channels," *accepted in 16th IEEE Int. Workshop on Signal Process. Adv. in Wireless Communications (SPAWC)*, Stockholm, Sweden, June 2015.

[29] C. Masouros, G. Zheng, "Exploiting Known Interference as Green Signal Power for Downlink Beamforming Optimization," *IEEE Transactions on Signal Processing*, July 2015

[30] S. Verdú, Spectral efficiency in the wideband regime, IEEE Trans. Inform. Theory, vol. 48, pp. 13191343, June 2002.

[31] M. C. Stefanovic and G. T. Djordjevic"BPSK and QPSK non-linear satellite communication system performance in the presence of cochannel interference," *Int. J. Satell. Commun. Network*; (DOI: 10.1002/sat.753), vol. 21 , no. 3, pp.285297, April 2003.

[32] F. Rusek, D. Persson, B. K. Lau, E. G. Larsson, T. L. Marzetta, O. Edfors, and F. Tufvesson, "Scaling up MIMO: Opportunities and Challenges with Large Arrays,"*IEEE Signal Processing Magazine*, Vol. 30, no. 1, pp.40-60, January, 2013.

[33] A. Checko, H.L. Christiansen, Yan Ying, L. Scolari, G. Kardaras, M.S. Berger, L. Dittmann, "Cloud RAN for Mobile NetworksA Technology Overview," IEEE Communications Surveys & Tutorials, Vol. 17, no. 1, pp. 405 - 426, First quarter, 2015.

[34] M. Alodeh, S. Chatzinotas and B. Ottersten,"Constructive Interference through Symbol Level Precoding for Multi-level Modulation," *IEEE Global Communications conference (Globecom)*, San Diego, CA, December 2015, available on Arxiv arXiv:1504.06750 [cs.IT].

[35] M. Alodeh, S. Chatzinotas and B. Ottersten,"Symbol-Level Multiuser MISO Precoding for Multi-level Adaptive Modulation: A Multicast View," *submitted*, available on arXiv, arXiv:1601.02788.

[36] E. Björnson, L. Sanguinetti, J. Hoydis, M. Debbah, "Optimal Design of Energy-Efficient Multi-User MIMO Systems: Is Massive MIMO the Answer?", arxiv http://arxiv.org/abs/1403.6150.

[37] S. Boyd, and L. Vandenberghe, Convex Optimization, Cambridge University press.

[38] J. Proakis, Digital Communications, 4th Edition.

Maha Alodeh (S'11, M'16) received her bachelor degree in electrical engineering from University of Jordan, Amman, Jordan in 2010, and her Ph.D. degree in electrical engineering from the Interdisciplinary center for Security and Trust, (SnT), University of Luxembourg in 2016. Alodeh's research interests includes signal processing for wireless and satellite communications with focus on interference management and cognitive radios.

Symeon Chatzinotas (S'06-M'09-SM'13)) received the M.Eng. in Telecommunications from Aristotle University of Thessaloniki, Greece and the M.Sc. and Ph.D. in Electronic Engineering from University of Surrey, UK in 2003, 2006 and 2009 respectively. He is currently a Research Scientist with the research group SIGCOM in the Interdisciplinary Centre for Security, Reliability and Trust, University of Luxembourg, managing H2020, ESA and FNR projects. In the past, he has worked in numerous R&D projects for the Institute of Informatics & Telecommunications, National Center for Scientific Research Demokritos, the Institute of Telematics and Informatics, Center of Research and Technology Hellas and Mobile Communications Research Group, Center of Communication Systems Research, University of Surrey. He has authored more than 120 technical papers in refereed international journals, conferences and scientific books. His research interests are on multiuser information theory, cooperative/cognitive communications and wireless networks optimization. Dr Chatzinotas is the co-recipient of the 2014 Distinguished Contributions to Satellite Communications Award, Satellite and Space Communications Technical Committee, IEEE Communications Society. He is currently co-editing a book on "Cooperative and Cognitive Satellite Systems" to appear in 2015 by Elsevier and he is co-organizing the First International Workshop on Cognitive Radios and Networks for Spectrum Coexistence of Satellite and Terrestrial Systems (CogRaN-Sat) in conjunction with the IEEE ICC 2015, 8-12 June 2015, London, UK.

Björn Ottesten (S'87-M'89-SM'99-F'04) was born in Stockholm, Sweden, in 1961. He received the M.S. degree in electrical engineering and applied physics from Linköping University, Linköping, Sweden, in 1986 and the Ph.D. degree in electrical engineering from Stanford University, Stanford, CA, in 1989.

Dr. Ottersten has held research positions at the Department of Electrical Engineering, Linköping University, the Information Systems Laboratory, Stanford University, the Katholieke Universiteit Leuven, Leuven, and the University of Luxembourg. During 96/97, he was Director of Research at ArrayComm Inc, a start-up in San Jose, California based on Ottersten' s patented technology. He has co-authored journal papers that received the IEEE Signal Processing Society Best Paper Award in 1993, 2001, 2006, and 2013 and 3 IEEE conference papers receiving Best Paper Awards. In 1991, he was appointed Professor of Signal Processing at the Royal Institute of Technology (KTH), Stockholm. From 1992 to 2004, he was head of the department for Signals, Sensors, and Systems at KTH and from 2004 to 2008, he was dean of the School of Electrical Engineering at KTH. Currently, he is Director for the Interdisciplinary Centre for Security, Reliability and Trust at the University of Luxembourg. As Digital Champion of Luxembourg, he acts as an adviser to European Commissioner Neelie Kroes.

Dr. Ottersten has served as Associate Editor for the IEEE Transactions on Signal Processing and on the editorial board of *IEEE Signal Processing Magazine*. He is currently editor in chief of *EURASIP Signal Processing Journal* and a member of the editorial boards of *EURASIP Journal of Applied Signal Processing* and *Foundations and Trends in Signal Processing*. He is a Fellow of the IEEE and EURASIP and a member of the IEEE Signal Processing Society Board of Governors. In 2011, he received the IEEE Signal Processing Society Technical Achievement Award. He is a first recipient of the European Research Council advanced research grant. His research interests include security and trust, reliable wireless communications, and statistical signal processing.